

STRESS CONCENTRATION AND VIBRATION MODAL ANALYSIS OF PROPELLER SHAFT USING FINITE ELEMENT ANALYSIS**Desejo Filipeson Sozinando¹, Bernard Xavier Tchomeni², and Alfayo Anyika Alugongo³**

Department of Industrial Engineering, Operations Management and Mechanical Engineering, Vaal University of Technology, Andries Potgieter Blvd, Vanderbijlpark, 1900, Private Bag X021, Vanderbijlpark, 1911, South Africa
¹desejos@vut.ac.za, ²bernardt@vut.ac.za, ³alfayoa@vut.ac.za

Date of Submission: 15th August 2023 Revised: 27th December 2023 Accepted: 08th January 2024**Abstract**

When propeller shafts are rotating and torque is transmitted through them, they are loaded with different kinds of stresses and vibrations. The propeller shaft can vibrate due to being unbalanced in the rotating assembly. The shaft has the possibility of stress concentration at some locations that might lead to failures or damage. Such points produce more stress than the surrounding areas. However, it should be made clear that vibration in combination with stress concentrations considerably reduces the performance and service life of the propeller shaft. To avoid resonance-related problems, finite element analysis (FEA) was used to conduct a linear dynamics analysis of first order characterized by natural frequencies and mode shapes. The effective mass factor is an outcome of modal analysis and informs how much mass participates in each mode and which modes are critical to causing damage. The results also demonstrate stress concentration zones, that is, critical points where high stress levels are possible, which may cause fatigue and structural failure. The resonance frequencies and effective mass participation factors indicated an increase in higher frequency modes and substantial mass involvement in the Y and Z directions.

Index Terms - Propeller shaft, modal analysis, mode shape, stress concentration, FEA.

INTRODUCTION

Propeller shafts are one of the most important elements when it comes to power transmission from an engine to a propulsion system, with a variety of uses in vehicles and across marine applications. A common problem associated with propeller shafts is the concentration of stress and vibration leading to shaft damage and failure. Proper design, balancing, and propeller shaft maintenance are also very important for optimal performance and longevity. The design and performance of propeller shafts are mainly influenced by vibration and stress concentration. These questions are raised in many studies, which aim to find ways to overcome them. The shaft amplitude vibrations have an increasing tendency with the operational speed, and the range of the critical speed of the shaft should be sidestepped to avoid resonance. The study also proposed that the implementation of a torsional damper could significantly decrease the vibration of the propeller shaft [1]. The spline root of the tooth yielded the highest stress concentration and the stress concentration factor increased with the transmitted torque on the shaft. This study proposes that a fillet radius, at the root of the spline, could be used effectively to reduce stress concentration [2]. Kumar et al. [3] proposed the methodology to optimize the propeller shatter design to reduce vibration and stress concentration. The shaft geometry was optimized by means of a genetic algorithm in the study, and it was found that the optimized design had less vibration and stress concentration than the original design. Another study on this topic was conducted by Hellum et al. [4] which analysed the influence of crack growth and geometries on the stress concentration of a propeller shaft. These improve geometry functions for the stress intensity factor of short semi-elliptical surface cracks subjected to stress mode. Lee et al. [5] studies the effect of eccentric propeller forces on the propeller shaft motion of a 50,000-deadweight tonnage. The results show that fluctuations in the shaft of the propeller have a significant influence on stability resulting in an imbalance of the loads on the bearing of the stern tube. Tchomeni and Alugongo [6] consider the transmission of non-linear signals and detect important crack features by synchronizing wavelet techniques in a propeller shaft system. The effect of propeller shaft damage is

reflected on motion transfer and point out Hooke's joint coupling compensating in the main source of instability [6-9]. Vijay et al. [10] considered the design and analysis of propeller shafts focusing on weight reduction and strength with FEA. It provides a comparison of solid and hollow shafts and considers the use of composite materials as a solution to better strength and weight reduction [10-13]. Niederwanger et al. [14] utilized composite propeller shafts comprising Aluminium alloy (2024 and 7068) and Titanium alloy (Ti-6Al-4V) as substitutions to conventional steel propeller shafts. Natural frequencies of a sectionalized pipeline gate valve were determined by Sozinando et al. [15] using modal analysis along with mode shapes and effective mass factors for such a pipeline gate valve using FEA. Ding et al. [16] employed modal frequency analysis to detect contact stiffness between the brake disc and the brake pads.

When Stress analysis is performed by entering loadings, boundaries, and material properties into a 3D model of the propeller shaft using FEA simulation that gives deformations and failure points in the model. The stress, displacement, and strain profiles are discussed in this paper. The general linear equations for the propeller shaft motion are established. and natural frequencies and mode shapes are determined. The modes, frequencies, and mass participation of different masses are analysed with particular emphasis on higher- and lower-order modes.

STRESS ANALYSIS OF PROPELLER SHAFT

In this section, the propeller shaft stress analysis implies the load application, restraints, and material properties on a 3D model of the shaft in order to determine how the stresses and deformations are distributed. The goal of the FEA is to forecast the locations of stress concentrations, deformations and failure points among the cross sections of the propeller shaft to ensure its integrity and optimal performance.

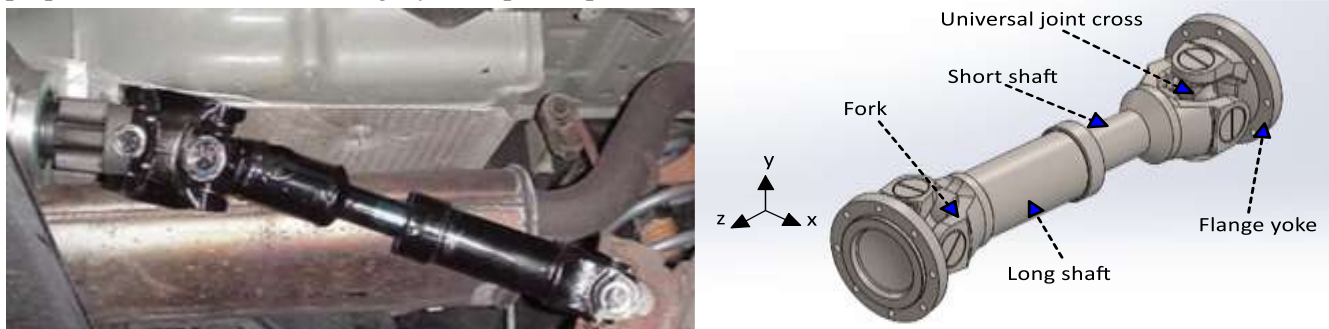


FIGURE 1 PHYSICAL SYSTEM AND 3D MODEL OF PROPELLER SHAFT

In Figure 1, the propeller shaft system is presented in an all-inclusive manner and is represented by its components. The shaft fork is the key component of the propeller shaft that connects all parts of the system, the long shaft that passes throughout the system, the short shaft used for power transmission, the flange yoke that ensures a perfect coupling, and the universal joint that allows flexibility and articulation.

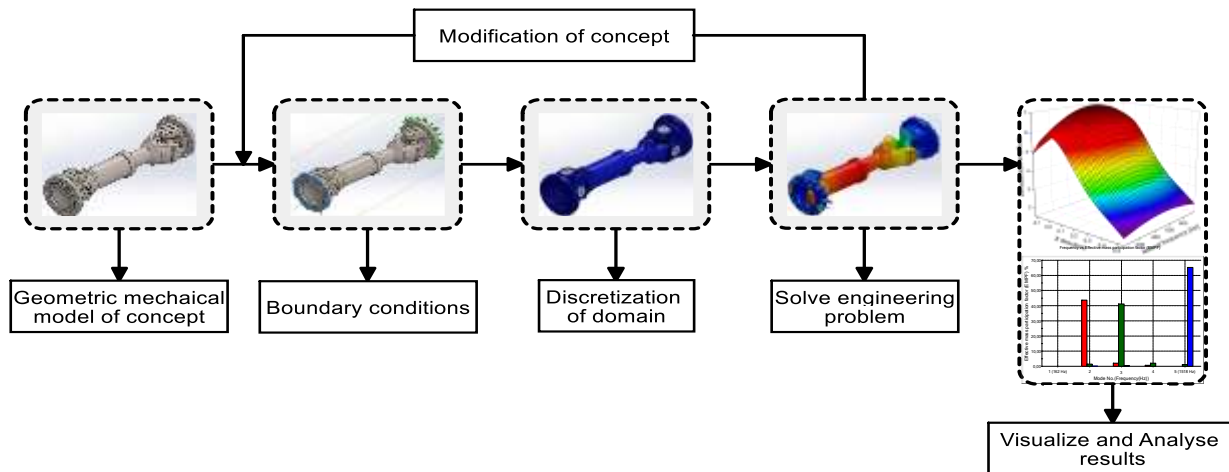


FIGURE 2 FLOW CHART OF THE METHODOLOGY IMPLIED IN THE FEA SIMULATION

As shown in Figure 2, the procedure flow chart for the FEA simulation is shown below. It starts with the input data, which flows through a set of vital steps sequentially. To begin with, we might define the structural geometry and material properties in order to provide a realistic picture of the entire system. A mesh generation procedure then follows which decomposes the complex geometries into finite element, enabling a through the analysis. The next step consists of the application of boundary conditions and loads that simulate real-world situations, allowing the assessment of the structural response in a repetitive way. Throughout the simulation, the FEA solver utilizes these inputs to produce outputs, which are stress distribution, displacement patterns, and the necessary data. Post-processing determines the simulation results; this is the process of examination and interpretation of it to position critical areas, stress concentrations, and potential failure points.

TABLE I MATERIAL PROPERTIES OF THE FEA MODEL

Material	Young's Modulus (GPa)	Density (kg/m ³)	Poisson's Ratio
Alloy	210	7700	0.28
Steel			

In this specific case, SolidWorks was used to perform a detailed analysis of the propeller shaft structure using a finite element technique which makes simulation and prediction of mechanical actions possible. Table 1 describes the characteristics of the materials that have been used in the FEA for the propeller shaft structure.

TABLE II DETAIL INFORMATION ABOUT THE MESH

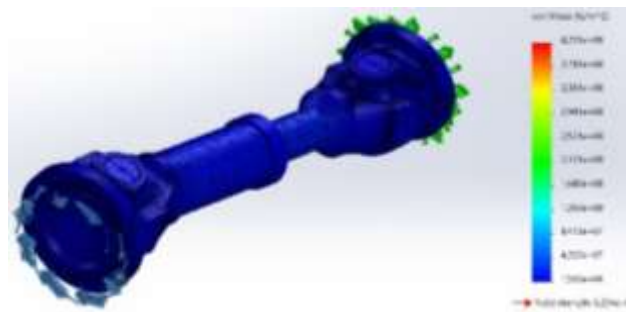
Mesh type	Solid Mesh
Mesher type	Blended curvature-based mesh
High-quality mesh based on Jacobian points	16 points
Maximum element size	25.4849 mm
Minimum element size	1.27424 mm
Quality of mesh	High

International Journal of Applied Engineering & Technology

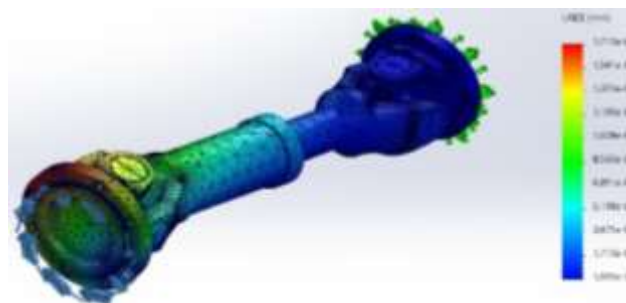
Table 2 shows specifications concerning the types of meshing applied in the FEA of the propeller shaft structure. The model is constructed with one solid mesh type which demonstrates that the structure is not equivalent to the shell and beam elements. The application of the curved-type mesh technique, which accounts for the geometry of the curvatures during the analysis, denotes the creation of a net with smooth edges and accurate appearances. Jacobian points can be used as landmarks to gauge the measure of quality in each mesh's element. An increased value of maximum element may be linked to the decrease of computational cost but, at the same time, it will have a negative impact on the accuracy. The problem may arise when dealing with concentrated stresses in complex geometrical details. On one hand, the advantages of higher spatial resolution of small minimum element size offer a better representation of fine details and local features for an accurate reproduction of the stress gradients or the geometric features included within the domain.

TABLE III STRESS, DISPLACEMENT, AND STRAIN PROFILE

Na me	Type	Min	Max
Stress	Von Mises Stress	15.60 kPa Node: 193332	420.1 MPa Node: 241937



Displacement	URES: Resultant Displacement	0.000 mm Node: 116430	0.171 mm Node: 51325
--------------	------------------------------------	-----------------------------	-------------------------



Strain	ESTRN: Equivalent Strain	7.076e ⁻⁸ Element: 125373	7.541e ⁻⁴ Element: 172259
--------	--------------------------------	--	--



In the FEA context, a colour indicative scale used in Table 3 provides a visual representation that allows inherent qualities of the obtained simulation results to be accomplished by emphasizing their magnitudes. This method is the application of colour mapping techniques which make the data capabilities proper and clear to see. The colour profile offers an extensive inspection of the distribution and severity of various factors such as stress, displacement, and strain throughout the examined propeller shaft structure.

MODAL ANALYSIS OF PROPELLER SHAFT

In this section, the implemented methodical approach would consist of an intensive study of the natural frequencies and normal modes present in the structure of the propeller shaft through finite element analysis. Focusing on the natural frequencies, from which natural vibrational frequencies of the structure are obtained, and the existing modes, where the corresponding shapes are described. Modulating a propeller shaft requires several fundamental assumptions and considerations.

- I. The material of the propeller shaft is assumed to behave linearly elastically. This means that the relationship between stress and strain is linear within the elastic range;
- II. The shaft experiences only small deformations and that plane cross sections remain plane and perpendicular to the deformed axis;
- III. Acclimated supported conditions are assumed at the ends of the shaft;
- IV. The propeller shaft is discretized into beam elements, and the finite-element model represents the shaft's behaviour using these elements;
- V. The modal analysis assumes that the mode shapes are orthogonal to each other to simplify the analysis and allow uncoupling of modes;
- VI. The linear superposition principle is applied, assuming that the total response of the system is a combination of individual modal responses.

The linear equation used to model the dynamics of the propeller shaft encapsulates the mathematical facts of the motion. It is computed by taking the product of inertia and dynamic stiffness, since it deals with two factors. The mass inertia matrix portrays the distribution of mass and how it determines the system response to changes in velocity, but the dynamic stiffness matrix describes the stiffness of the system and how it behaves under the influence of force or displacements. Expressed in a general linear form, the motion equation for the propeller shaft can be written as

$$[M] \{\ddot{u}\} + [K] \{u\} = \{0\} \quad (1)$$

The inertia matrix M is the one that stands for mass, and the stiffness matrix K represents spring. Assuming displacement varies harmoniously with time, displacement u and acceleration \ddot{u} are expressed as follows:

$$\{u\} = \{\phi\}_i \sin(\omega_i t + \theta_i) \quad (2)$$

$$\{\ddot{u}\} = -\omega_i^2 \{\phi\}_i \sin(\omega_i t + \theta_i) \quad (3)$$

The modal displacement vector $\{\phi\}_i$ can be calculated by substituting (2) and (3) into (1) yields

$$([K] - \omega_i^2 [M]) \{\phi\}_i = \{0\} \quad (4)$$

As a result of (4), it is possible to calculate the natural frequency f_i as follows:

$$f_i = \frac{\omega_i}{2\pi} \quad (5)$$

The shaft structures of the propeller respond to the varying dynamic loading depending on the participation factor and the effective mass. Assuming that the mass moves in the X, Y, and Z directions, the participation factor is as follows:

$$\gamma_i = \{\phi\}_i^T [M] \{\lambda\} \quad (6)$$

Based on the global Cartesian directions, it is possible to calculate the displacement spectrum $\{\lambda\}$ in each direction, as well as the rotation about each axis.

KERNEL DENSITY ESTIMATION

Kernel Density Estimation (KDE) is a non-parametric technique which is useful for estimation of the probability density function of a random variable. In this setting we model X variable as sample (X_1, X_2, \dots, X_n) , where each is an independent and equal-sized draw from the univariate distribution, unknown at x. Each sample is determined by its own sample size. Implementation of KDE allows FEA data to be analyzed to determine the probability density of deformation modes for each direction (X, Y, Z). By using the KDE analysis, the most likely direction (X, Y, Z) for particular deformation modes can be defined as

$$f(x) = \frac{1}{nh} \sum_{i=1}^n K \left\{ \frac{1}{h} (x - x_i) \right\} \quad (7)$$

$$h = \left(\frac{4\sigma^5}{3n} \right) \quad (8)$$

where σ is the standard deviation of the input data, and n is the number of samples in the input data.

$$K(x) = (2\pi)^{-\frac{1}{2}} \exp\left(-\frac{x^2}{2}\right) \quad (9)$$

International Journal of Applied Engineering & Technology

The function $K(x)$ represents the kernel of normal form, a non-negative function, and h is the smoothing parameter with a value greater than 0, also known as the bandwidth. The optimal form of h can be found with equation (8), which is a scaled version of the kernel. When choosing h , it is ideal to make it as small as the data permits, but this decision is always accompanied by a trade-off between the estimator's bias and its variance. This balance is crucial for achieving optimal results.

TABLE IV VIBRATION MODE SHAPE




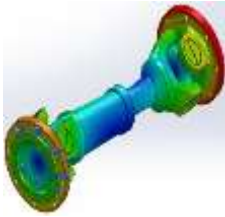

Mode Shape: 1 Value = 88.8406 Hz	Mode Shape: 2 Value = 97.872 Hz	Mode Shape: 3 Value = 149.634 Hz	Mode Shape: 4 Value = 160.331 Hz	Mode Shape: 5 Value = 286.782 Hz
				
Resultant Amplitude $1.058e^{-1}$ mm Node 1292	Resultant Amplitude $6.840e^{-2}$ mm Node 1427	Resultant Amplitude $1.954e^{-1}$ mm Node 12218	Resultant Amplitude $1.560e^{-1}$ mm Node 12110	Resultant Amplitude $2.024e^{-1}$ mm Node 11840

Table 4 shows the primary mode of vibration of the engine-shaft system, equal to 88.8406 Hz, representing the natural or resonant frequency of the system that the system tends to oscillate most easily. The second mode presents a frequency slightly higher than the natural one of 97.872 Hz, thus suggesting an additional natural vibrational pattern within the system. The 3rd mode shows the increase of the frequency to 149.634. indicating a more complex vibration in the propeller resulting in the strengthening of the frequency. This results in a need for rigorous assessment of the system's capability to accept increased frequency of operation. Again, the trend of rising frequencies increases the amplitude of the fourth-mode frequency, which amounts to 160.331 Hz. The 5th model having the highest resonant frequency of 286.782 Hz exhibits more vigorous oscillatory behaviour.

TABLE V MASS PARTICIPATION (NORMALIZED)

Mode Number	Frequency (Hz)	X direction	Y direction	Z direction
1	88.841	$1.8274e^{-6}$	0.71748	$2.9958e^{-5}$
2	97.872	$1.5252e^{-7}$	$3.4946e^{-5}$	0.81758
3	149.63	0.14462	0.00059885	$6.7394e^{-7}$
4	160.33	0.00062441	0.10461	$4.5468e^{-6}$
5	286.78	$2.3448e^{-5}$	$2.6013e^{-6}$	$8.0217e^{-7}$
		Sum X = 0,14527	Sum Y = 0.82273	Sum Z = 0.81761

In Table 5 lies the participation mass (normalized) covering different modes of the propeller shaft structure. Identified mode numbers are written on each row of the table with a corresponding mode of vibration. The column frequency stands for the natural frequency obtained which corresponds to each mode in Hz. Natural frequencies are of importance because they represent the system's innate tendency to vibrate at certain specific rates. The X, Y, and Z axis constitute the normalized mass participation projections in each modality that is depicted on the respective axes. These ratios hence correspond to the percentages of the mass that is involved in each mode of vibration in the directions indicated.

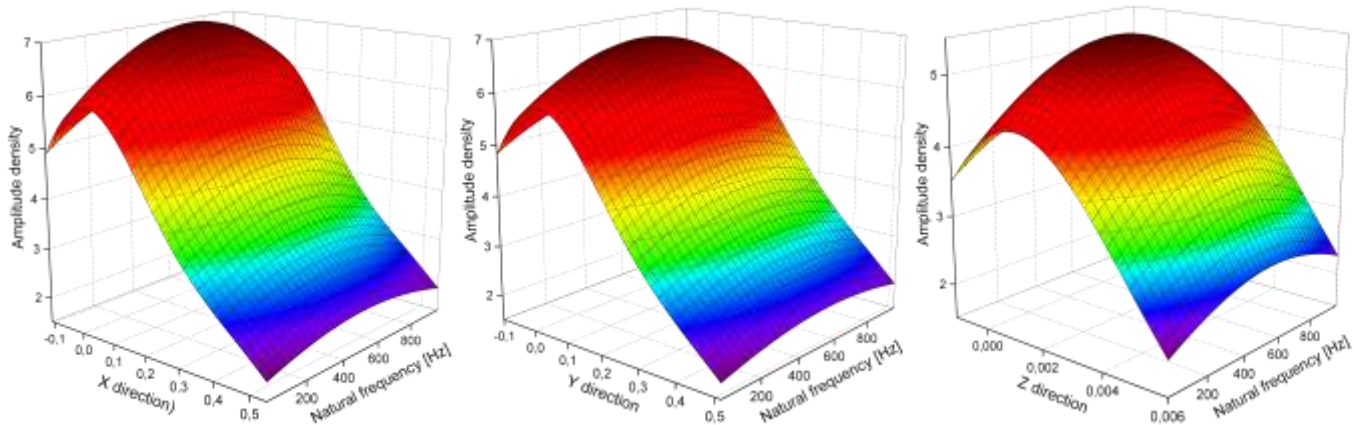


FIGURE 3 3D KERNEL DENSITY ESTIMATION: (A) X-DIRECTION; (B) Y-DIRECTION; (C) Z-DIRECTION

Figure 3 (A), (B) and (C) illustrates a 3D grid density estimation influenced by deformation modes from discrete vectors of X, Y and Z directions. The investigated kernel density estimation (KDE) methods were employed in this section as visualization technique for propeller shaft system deformations as an initial step to aid the identification of influencing directions, only using node connectivity information. Inverse bounding was used to avoid the traditional Gaussian distribution without considering the geometric nature and the shapes of the cubic distribution. To compensate for the KDE limitations of sensitive parameter estimation, a kernel bandwidth rules estimation technique was applied to consider the effect of the kernel bandwidth.

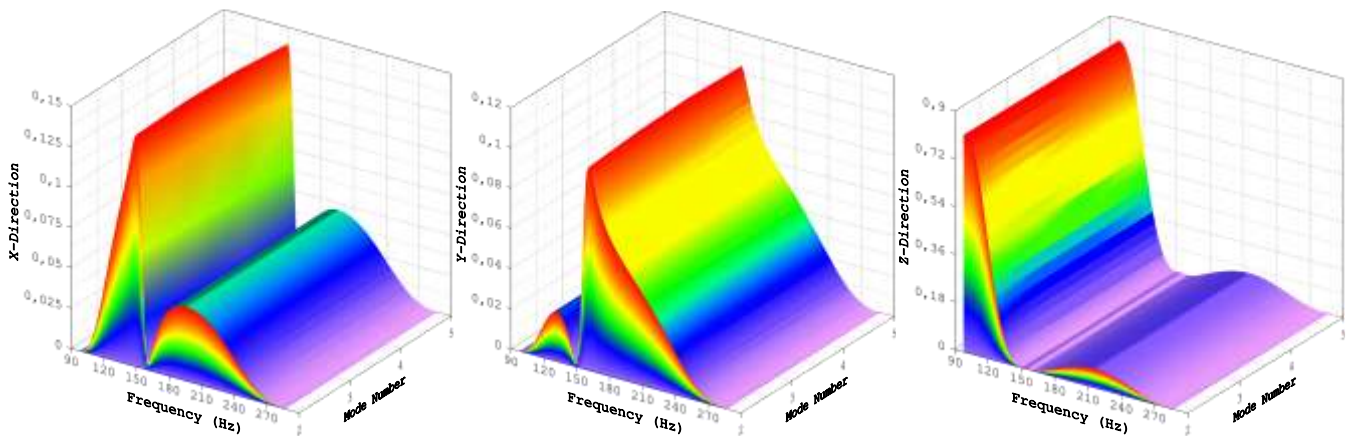


FIGURE 4
3D WATERFALL OF MASS PARTICIPATION FACTOR: (A) X-DIRECTION; (B) Y-DIRECTION; (C) Z-DIRECTION

Figure 3 illustrates a 3D waterfall plot, which indicates that the classes of mass participation characteristics influence the frequency and modes of the X, Y, and Z directions. In Figure 4(A) are a number of frequencies and modes that almost differ from each other, depicted as a line with a consistent orientation on the X-axis. The peak of 0.14462 represents the most dominant participation factor in the X-direction. Also, the participation pattern depicted in Figure 4(B) is rather a mass in the Y direction with mode number and frequencies. The plane yields a high value of 0.71748 which implies a huge effect on the structure response in the Y direction of the propeller at specific mode and frequency. Figure 4(C) depicts the specifics of the Z-axis, where structural vibration is focused on a certain mode and frequency, taken in the direction of the structure. The first major mass fraction of the participation factor taken in the Z direction, a value of 0.81758, implies the most influencing response of the propeller shaft system.

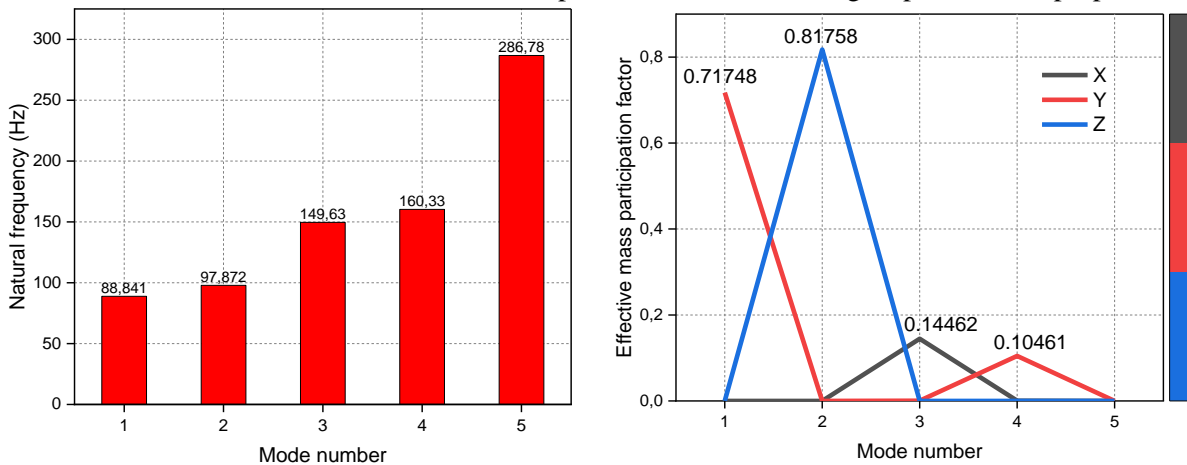


FIGURE 5
(A) RESONANCE FREQUENCIES; (B) EFFECTIVE MASS PARTICIPATION FACTOR

Figure 5(A) illustrates the natural frequencies corresponding to each mode of vibration. The detected trend, including intensification of cycles from the first mode, with frequency value 88.841 Hz, to the fifth mode, with frequency value 286.78 Hz, shows the increase in the higher mode frequencies, which reflects an increase in the speed of the oscillations in the shaft system of the propeller. Figure 5(B) refers to the effective participation of the mass for each mode. The fact that the mass participation in the event is tied to the directions Y and Z is clearly

illustrated in the graph. The fact that these modes are active in vibrations that involve a considerable part of the structure's mass along the Y and Z axes. The less participation in the X direction gives the idea that vibrations in that direction are relatively smaller in the global structural response.

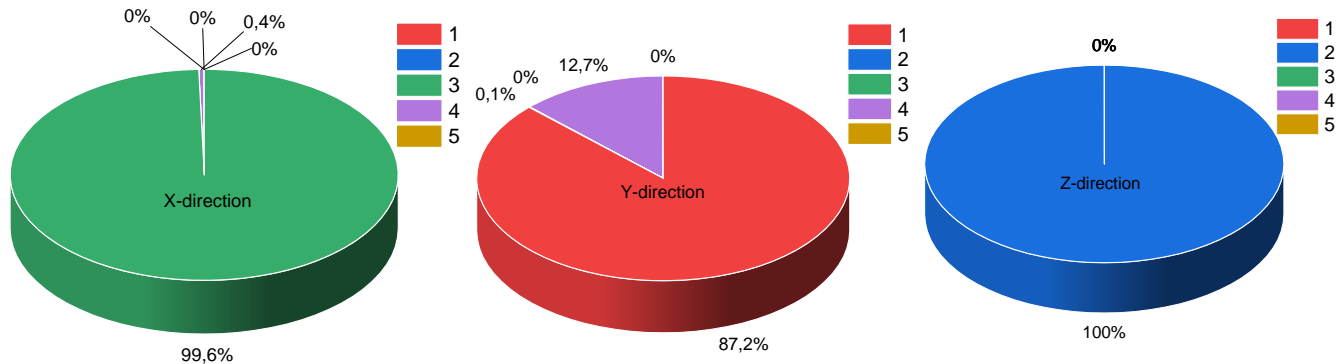


FIGURE 6
PERCENTAGE OF MASS PARTICIPATION OF EACH MODE

As Figure 6 shows, each of these modes has a different percentage of mass participation, which can be seen to have a greater amount of mass with that mode under an actual excitation direction. These quantities are noted as a fraction or a percentage of the total system mass, and this shows the balance of mass in the system. It is noticeable that in the X-direction, 99.6% of mass participation is amassed in the 3rd mode. But in the Y-direction the movement shows up in the 1st mode of 87.2% of the interactions and the in the Z-direction the 2nd mode has 100% of the interactions. However, modes 4 and 5 exhibit lower mass participation, making them less preferable as failure modes.

CONCLUSION

Stress concentrations at specific points along the propeller shaft pose a risk of potential failures or damages. Recognizing that such stress concentrations can induce higher stress levels than in surrounding areas. The results of the analysis revealed key locations prone to high-stress displacement and strain levels, which pose a risk of fatigue and structural failure. The resonance frequencies and effective mass participation factors indicated a noticeable increase in higher mode frequencies and highlighting the substantial mass involvement in the Y and Z directions. The first three modes are identified as having a high potential to cause damage to a propeller shaft structure. The frequencies are noted to have an increasing pattern and participation associated with these modes. It becomes evident that factors such as higher stress levels, resonance frequencies, and effective mass participation can significantly impact the performance of propeller shaft.

ACKNOWLEDGMENT

Authors acknowledge the technical assistance offered by the Department of Industrial Engineering, Operations Management, and Mechanical Engineering at Vaal University of Technology.

REFERENCES

- [1] Song, Haiqin, Jinfeng Zhang, and Fan Zhang. "Rotor strength and critical speed analysis of a vertical long shaft fire pump connected with different shaft lengths." *Scientific reports* 12, no. 1 (2022): 9351.
- [2] Wu, Yuzhong, Yilong Liang, Cunhong Yin, Fengtai Zhang, Baolai Chen, Songyun Yang, Xichang Shang, and Jianghe Zou. "Analysis of factors affecting the wear failure of an aeroengine spline pair and evolution mechanism of the tribolayer." *Engineering Failure Analysis* 146 (2023): 107113.

- [3] Kumar, G. Suresh, and L. A. Kumaraswamidhas. "Design optimization focused on failures during developmental testing of the fabricated rear-axle housing." *Engineering Failure Analysis* 120 (2021): 104999.
- [4] Hellum, Vidar, Tom Lassen, and Andrea Spagnoli. "Crack growth models for multiaxial fatigue in a ship's propeller shaft." *Engineering Failure Analysis* 127 (2021): 105470.
- [5] Lee, J. W., Vuong, Q. D., Jeong, B., & Lee, J. U. (2022). Changes in propeller shaft behavior by fluctuating propeller forces during ship turning. *Applied Sciences*, 12(10), 5041.
- [6] Tchomeni, B. X., & Alugongo, A. (2021). Modelling and dynamic analysis of an unbalanced and cracked cardan shaft for vehicle propeller shaft systems. *Applied Sciences*, 11(17), 8132.
- [7] Shen, C., & Lu, C. (2021). A refined torsional-lateral-longitude coupled vehicular driveline model for driveline boom problems. *Applied Mathematical Modelling*, 90, 1009-1034.
- [8] Bharti, S. K., Sinha, A., Samantaray, A. K., & Bhattacharyya, R. (2021). Dynamics of a rotor shaft driven by a non-ideal source through a universal joint. *Journal of Sound and Vibration*, 499, 115992.
- [9] Bharti, S. K., & Samantaray, A. K. (2021). Resonant capture and Sommerfeld effect due to torsional vibrations in a double Cardan joint driveline. *Communications in Nonlinear Science and Numerical Simulation*, 97, 105728.
- [10] Vijay, A., Vinayan, M. P., Hafsana, A., & Jagadeesha, T. (2022). Design, Fatigue Analysis, and Optimization of Propeller Shafts Using Finite Element Analysis. In *Recent Advances in Manufacturing Modelling and Optimization: Select Proceedings of RAM 2021* (pp. 241-251). Singapore: Springer Nature Singapore.
- [11] Saravanakumar, S., K. Kalaiselvan, M. Ramesh, K. B. Prakash, A. Sundar Rajan, T. Subash Chandru, and M. S. Aravinth. "Design and comparison of the strength of propeller shaft for truck made of AA2024, AA7068, and Ti-6Al-4V using ANSYS." *Materials Today: Proceedings* 69 (2022): 1442-1454.
- [12] Oh, H., Myung, N., & Choi, N. S. (2016). Fatigue life analysis and prediction of 316L stainless steel under low cycle fatigue loading. *Transactions of the Korean Society of Mechanical Engineers A*, 40(12), 1027-1035.
- [13] Gezu, L., Nallamotheu, R. B., Nallamotheu, S. K., Nallamotheu, A. K., & Tafesse, D. (2021). Design and analysis of composite drive shaft for rear-wheel-drive vehicle. In *Recent Advances in Sustainable Technologies: Select Proceedings of ICAST 2020* (pp. 83-92). Springer Singapore.
- [14] Niederwanger, A., Ladinek, M., Lang, R., Timmers, R., & Lener, G. (2019). On the stability and sensitivity of the strain-life approach using the example of mild steel. *Journal of Constructional Steel Research*, 153, 483-494.
- [15] Sozinando, D. F., Tchomeni, B. X., & Alugongo, A. A. (2023). Modal Analysis and Flow through Sectionalized Pipeline Gate Valve Using FEA and CFD Technique. *Journal of Engineering*, 2023.
- [16] Ding, Haizhou, Qiang Zhu, and Hongming Lyu. "Identification of Contact Stiffness between Brake Disc and Brake Pads Using Modal Frequency Analysis." *Journal of Engineering & Technological Sciences* 52.4 (2020).

AUTHOR INFORMATION

Desejo Filipeson Sozinando, Lecturer, Department of Industrial Engineering, Operations Management and Mechanical Engineering, Vaal University of Technology, Vanderbijlpark.

International Journal of Applied Engineering & Technology

Bernard Xavier Tchomeni, Associate Professor, Department of Industrial Engineering, Operations Management and Mechanical Engineering, Vaal University of Technology, Vanderbijlpark.

Alfayo Anyika Alugongo, Professor, Department of Industrial Engineering, Operations Management and Mechanical Engineering, Vaal University of Technology, Vanderbijlpark.